Molecular Sieving on the Surface of a Protein Provides Protection Without Loss of Activity

*Mi Liu, Pasquale Tirino, Milos Radivojevic, Daniel J. Phillips, Matthew I. Gibson, Jean-Christophe Leroux, and Marc A. Gauthier**

Tethering polymers to surfaces represents the cornerstone of a wide range of applications, including the stabilization of colloids/biomolecules and the preparation of functional coatings. Unfortunately, despite the prevalence of protein-tethered polymers in the pharmaceutical sector, the analysis of such polymer monolayers on a molecular level is difficult. In this work, simple ^{1}H NMR spectroscopy and the catalytic properties of α-chymotrypsin are used to analyze the conformational/permeability properties of protein-bound monolayers of poly(oligoethyleneglycol monomethylether methacrylate) (pOEGMA), a biocompatible comb-polymer of interest in the biomedical field. By analyzing >100 distinct conjugates of α-chymotrypsin and pOEGMA, a detailed picture of the behavior of pOEGMA on the surface of a protein was obtained. Remarkably, control of polymer conformation and inter-penetration produced a thus far overlooked molecular sieving effect. The application of this effect for the "smart" PEGylation of proteins is portrayed, from which insight is provided for the design of other therapeutic bioconjugates and functional coatings with selective permeability properties.

1. Introduction

Tethering polymers to surfaces represents the cornerstone of a wide range of applications, including the stabilization of colloids/biomolecules and the preparation of functional coatings.[1] For instance, the modification of therapeutic proteins with monolayers of linear poly(ethylene glycol) (PEG), a process referred to as PEGylation, is the current benchmark for increasing protein stability and for prolonging their circulation lifetime.[2] In many cases, the relative permeability of molecules through the polymer monolayer towards the surface is a crucial design parameter influencing efficacy. For example, PEG monolayers grafted to L-asparaginase, an enzyme used for the treatment of acute lymphoblastic leukemia,[3] should reject proteins from the immune system while simultaneously permitting the facile transit of the small substrate L-asparagine to the enzyme's active site.[2,4] Unfortunately, despite the prevalence of protein-tethered polymers in the pharmaceutical and biomedical sector, a detailed analysis of the permeability properties of such monolayers is difficult.[5]

In this work, simple ^{1}H NMR spectroscopy and the catalytic properties of α-chymotrypsin (αCT) were used to analyze the conformational/permeability properties protein-bound monolayers of poly(oligoethyleneglycol monomethylether methacrylate) (pOEGMA), a biocompatible polymer of current interest.[6] pOEGMA is an emerging comb-shaped derivative of PEG that possesses unique conformational properties which have lead to its use in peptide/protein PEGylation[7] and for the development of effective nonfouling coatings.[1g,1h] For instance, while PEG adopts a random coil conformation in solution, comb-polymers can behave either as compact ellipsoids or as (semi) rigid cylinders as a function of backbone and side-chain lengths.[8] Based on its solution behavior, it is hypothesized herein that the aspect ratio of pOEGMA can be accurately tuned on the surface of a protein to generate well-defined monolayers with potentially distinct permeability characteristics.

The conformation and packing of protein-bound pOEGMA monolayers was conveniently analyzed through >100 unique conjugates of pOEGMA and αCT by ^{1}H NMR spectroscopy and was correlated to the permeability characteristics of the polymer monolayer, established using the particular bioanalytical characteristics of αCT. More specifically, this protein displays catalytic activity towards substrates of differing size, which can be used to probe the influence of size on ease of access to the enzyme's catalytic site. Through the detailed molecular picture of the behavior of pOEGMA on the surface of a protein, new insight into the design of other therapeutic bioconjugates and non-fouling coatings with selective permeability properties is provided, which are of use in broad fields of application.

M. Liu, P. Tirino, M. Radivojevic,
Prof. J.-C. Leroux, Dr. M. A. Gauthier
Swiss Federal Institute of Technology Zürich (ETH Zürich)
Department of Chemistry and Applied Biosciences
Institute of Pharmaceutical Sciences
Wolfgang-Pauli Str. 10, 8093 Zürich, Switzerland
E-mail: M.A.G.marc.gauthier@pharma.ethz.ch
P. Tirino
Department of Chemistry "Paolo Corradini"
University Federico II
Via Cinthia, I-80126 Naples, Italy
D. J. Phillips, Prof. M. I. Gibson
Department of Chemistry
University of Warwick
Gibbet Hill Road, Coventry, UK

DOI: 10.1002/adfm.201202227

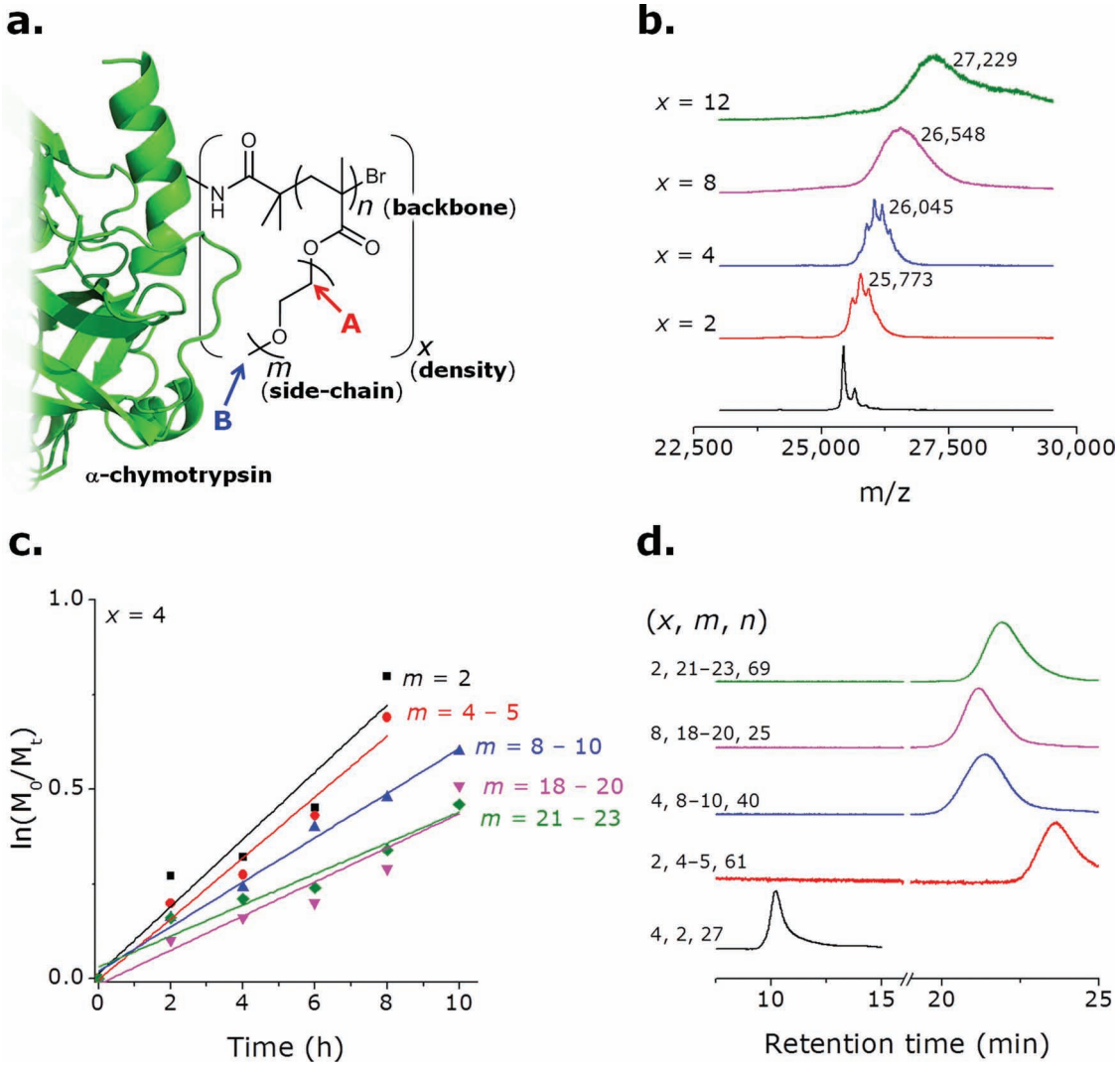

Figure 1. a) 3D parameter space (*x*, *n*, *m*) of αCT–pOEGMA conjugates. >100 unique αCT–pOEGMA conjugates were prepared by activation of αCT with 2-bromoisoburyryl bromide and in situ growth of pOEGMA chains by atom transfer radical polymerization. Analysis of prepared b) αCT macro-initiators and c,d) αCT–pOEGMA conjugates. b) Analysis of the molecular weight of αCT macro-initiators by MALDI-TOF MS to determine the average number of initiating groups covalently attached to the protein; c) Kinetics of the ATRP process. The polymerization reaction showed the characteristics of a living polymerization reaction with pseudo-first-order kinetics. In the figure, typical results obtained for $x = 4$ and the entire series of OEGMA monomers examined are presented. d) Typical SEC chromatograms of αCT–pOEGMA conjugates. All conjugates tested displayed monomodal molecular-weight distributions. Note that in this figure, all chromatograms were recorded in aqueous media, with the exception of the conjugate with $m = 2$, which was measured in DMF.

2. Packing and Conformation of pOEGMA within Protein-Bound Monolayers

As first reported by Matyjaszewski and co-workers,[9] a series of pOEGMA–protein conjugates were prepared by in situ growth of polymer chains directly from the surface of αCT (**Figure 1**a) by atom transfer radical polymerization, a powerful tool for the preparation of well-defined polymers and nanostructures.[10] This process yielded >100 well-defined conjugates with unique combinations of grafting density (*x*; number of polymer chains per protein), backbone length (*n*), and side-chain length (*m*) (Table S1–S8 in the Supporting Information). The grafting density was precisely varied ($x = 2$, 4, 8, and 12; Supporting Information Figure S1, Figure 1b) by controlling the number of initiating groups on the surface-exposed lysine residues of the protein. Digestion of the protein macro-initiators with trypsin followed by mass spectrometry failed to identify specific peptides preferentially modified with initiating groups (data not shown), suggesting random modification of the surface of αCT. The length of the oligoethylene glycol side-chain ($m = 2$, 4–5, 8–10, 18–20, and 21–23 oxyethylene units) was varied by selecting the appropriate OEGMA monomer, and the backbone length was varied between $n \approx 10$–100 monomeric units by sampling the living polymerization reaction at different times (Figure 1c, d). The conjugates were digested with pepsin, which is a more aggressive protease than trypsin and has the feature

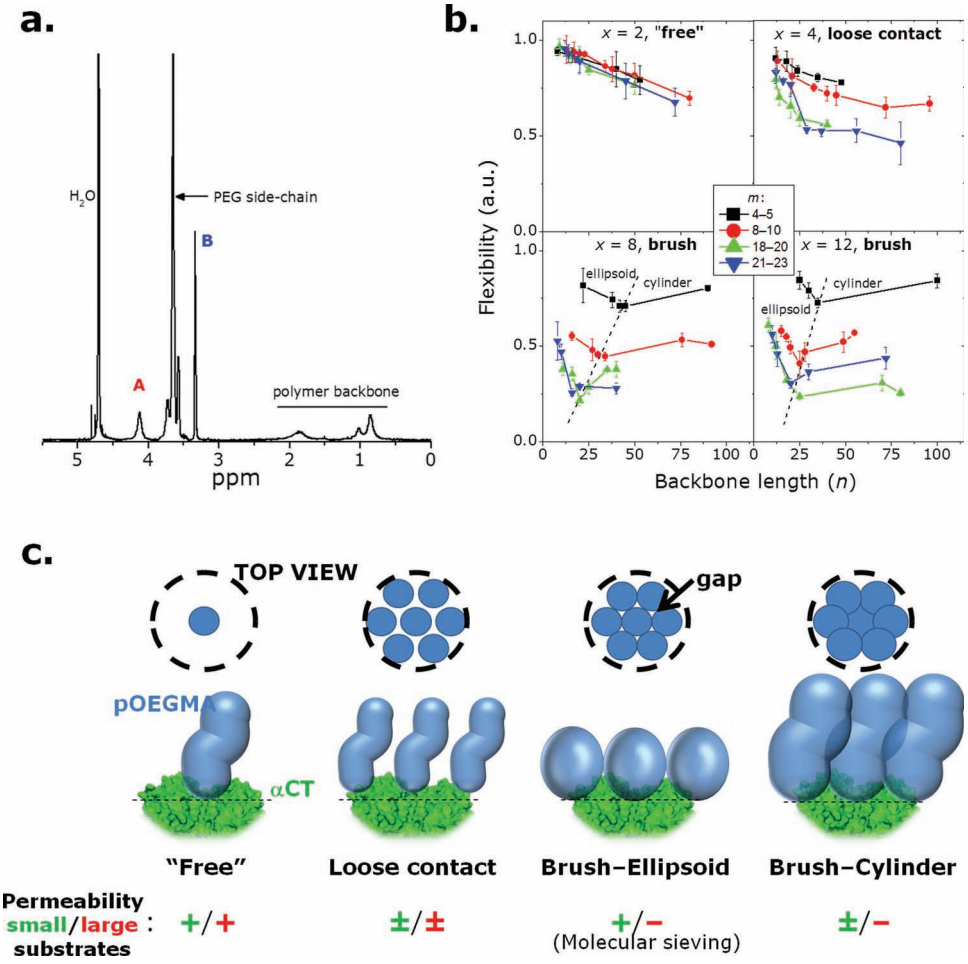

Figure 2. a) Analysis of backbone flexibility. Representative ^{1}H NMR spectrum of an αCT–pOEGMA conjugate for which polymer backbone flexibility was probed through the integral of peak A (proton at A in Figure 1a), normalized to the integral of peak B (proton at B in Figure 1a), which corresponds the most solvated and mobile group on pOEGMA. b) Conformation of protein-bound pOEGMA monolayers. Polymer backbone flexibility estimated by ^{1}H NMR spectroscopy provides insight into the conformation and organization of pOEGMA within protein-bound monolayers. Increasing grafting density led to a pronounced loss of flexibility signaling a transition from highly mobile pOEGMA chains ($x = 2$) to a dense brush-like pOEGMA monolayer ($x \geq 8$). In the brush regime, it is hypothesized that transitions of the pOEGMA chains from ellipsoidal to cylindrical take place to minimize inter-chains interactions within the monolayer. Mean ± SD (n = 3). c) Cartoon illustrating the idealized organization and selective permeability characteristics of the four different regimes observed within the 3D parameter space of protein-bound pOEGMA examined.

of being able to hydrolyze amide bonds within proteins but not ester bonds.[11] This digestion produced pOEGMA–peptide fragments (Supporting Information Figure S2) with an average molecular weight consistent with the molecular weight of the parent αCT–pOEGMA conjugate divided by the number of initiator groups. This suggests that initiation of polymerization occurred at all expected sites on the protein, and the all polymer chains have comparable lengths (monomodal distribution).

To analyze the conformation and packing of pOEGMA on the surface of the protein, the flexibility of the polymer backbone was probed by ^{1}H NMR spectroscopy. It is commonly observed that a decrease of molecular mobility leads to a loss of signal due to changes of the characteristic relaxation times of protons within the polymer.[12] Thus, a simple ^{1}H NMR spectrum recorded under typical conditions used for small molecules contains semi-quantitative information on the average (relative) flexibility at different locations on the polymer without the hassle of a more laborious analysis of the actual relaxation times and their distribution within a given polymer. This feature was exploited herein to compare the relative flexibility of the first side-chain methylene group adjacent the polymer backbone (Peak A, in **Figure 2**a) versus the terminal methyl group on the side-chains (Peak B, in Figure 2a), which is expected to be the most solvated and free group on pOEGMA. A dimensionless flexibility factor F, defined as $F = A \div 2/3B$, was calculated for each conjugate. F can vary from a value of 1 for a fully flexible and solvated polymer backbone and tend towards 0 when it is rigid, extended, and/or collapsed.

At low grafting density ($x = 2$) flexibility was initially high ($F \approx 1$) and decreased linearly with n, independently of side-chain length (Figure 2b). This suggests that the protein-tethered polymer chains are essentially "free" and behave independently of one another on the surface of the protein (Figure 2c). At this grafting density, conformational changes from ellipsoid to cylinder, while expected based on the behavior of related polymers,[8] did not lead to a discernible feature in the graph of F versus n.

At intermediate grafting density ($x = 4$) F was again initially high (≈1) at low n, indicating that the chains remain loosely spread on the surface of the protein. As n increased, a more pronounced decrease of F compared to that observed for $x = 2$ was observed due to partial contact between the polymer chains. The decrease of flexibility was more pronounced for polymers with longer side-chain lengths m, as expected from the larger "footprint" of these polymers. Globally, the polymer chains are in a "loose contact" regime (Figure 2c) whereby interactions between protein-bound pOEGMA chains partially restrict their freedom.

At high grafting density ($x = 8$, 12), the initial flexibility of the backbone (at low n) was $0.5 < F < 0.8$, signaling strong contact between the pOEGMA chains. Such interactions should force the longest dimension of the polymer along an axis perpendicular to the surface, i.e., the so-called brush regime for surface-tethered polymer monolayers.[13] F strongly decreased linearly versus n to a minimal value at n = 20–40, then increased linearly at a more moderate slope with respect to n (Figure 2b). This plot provided an indication that at this minimal value, pOEGMA changes conformation to minimize inter-polymer contacts. Indeed, conformational differences as a function of n have been observed for other comb-polymers such as poly(styrene)-*g*-oligo(ethylene glycol), which undergo ellipsoid to cylinder transitions with increasing n.[8] The putative interpretation put forth herein is that the pOEGMA chains, which initially behave as compact and non-interpenetrated ellipsoids at low n, change conformation to cylinders beyond n = 20–40. This slightly decreases the footprint of the polymer on the surface of the protein, but promotes side-chain interpenetration between neighboring chains. For dilute solutions of poly(styrene)-*g*-oligo(ethylene glycol), such a transition has been shown to occur between n = 8–40,[8] a value which is compatible with the interpretation put forth above. The n at which the transition from ellipsoid to cylinder was observed herein decreased with increasing m as well as increasing x (dashed lines in Figure 2b), which corroborates the interpretation that confinement of the pOEGMA chains within the dense monolayer is driving the change of backbone conformation.

3. Selective Permeability of Protein-Bound pOEGMA Monolayers

αCT displays catalytic activity towards substrates of differing size. Consequently, analysis of the activity of αCT–polymer conjugates towards substrates including a single amino acid derivative (benzoyl-L-tyrosine *p*-nitroanilide (BT*p*NA), 405 Da), to a peptide (*N*-Succinyl-Ala-Ala-Pro-Phe *p*-nitroanilide, 625 Da), to a protein (casein, 19–25 kDa) provides information on the relative ease of diffusion of the substrates towards the active site of αCT within the conjugate. Note that the catalytic site on αCT is the same for all three substrates. Hydrolysis of all three substrates involves cleavage of an amide bond, and the substrates differ significantly in molecular weight. To identify regions of preferential activity towards smaller substrates, an "activity ratio" was calculated by dividing the activity of the conjugates towards either BT*p*NA (**Figure 3**a) or the peptide substrate (Figure 3b) by the activity towards casein, all measured using established protocols based on the kinetics of substrate hydrolysis. An alternative presentation of data can be found in Supporting Information Figure S3. The raw activity values for all conjugates towards all substrates can be found in Supporting Information Table S1–S8 and are plotted as a map in Figure S4.

At low grafting density ($x < 8$; i.e., in the "free" and loose contact regimes), none of the conjugates displayed any particular preference for small or large substrates, as indicated

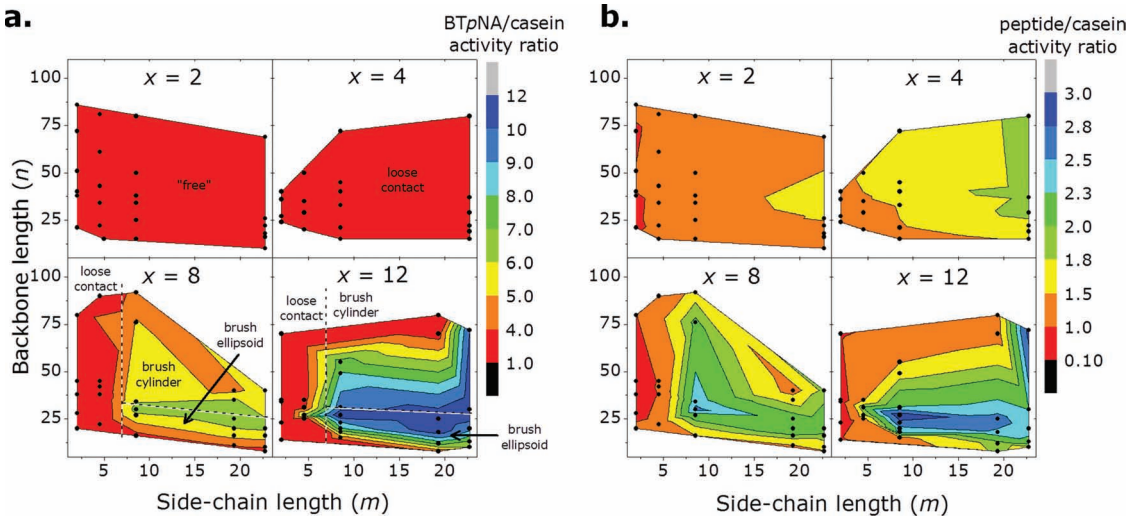

Figure 3. Molecular sieving of protein-bound pOEGMA monolayers. Regions of preferential activity towards small substrates such as a) BT*p*NA or b) peptide compared to large substrates (casein), were observed at room temperature by comparing the relative activities of each individual conjugate towards the three substrates. For $x \geq 8$, the brush–ellipsoid regime determined by NMR spectroscopy coincides with regions showing strong preferential activity towards small substrates (in blue). Color maps established as linear projections between data-points (black dots are the mean of n = 3). Absolute activity values are found in Supporting Information Table S1–S8 and Figure S5 as Mean ± SD (n = 3).

by activity ratios close to 1 (Figure 3a,b top). However, at high grafting density (x = 8, 12; i.e., in the brush regime) a zone of preferential activity towards small substrates was observed for n < ≈35–40 (Figure 3a,b bottom). In this region, the preferential activity ratio reached a maximum of ≈10 for BT*p*NA ÷ casein and ≈3 for peptide ÷ casein. Interestingly, this zone (defined by x, n, and m) coincided with the pOEGMA monolayer being in a brush–ellipsoid conformation (Figure 2b) and was observed for both BT*p*NA and the peptide substrate, indicating that this phenomenon does not result from specific substrate–conjugate interactions. The lower preferential activity ratio observed for the peptide substrate (versus BT*p*NA) further points to a size-dependence of the phenomenon. From these experiments, it appears that protein-bound pOEGMA monolayers in brush–ellipsoid conformation possess pronounced selective permeability, or "molecular sieving" properties. Similar results were obtained at 37 °C (Supporting Information Figure S5).

4. Phenomenological Interpretation

The "molecular sieving" properties observed in the brush–ellipsoid regime result from the formation of a densely packed monolayer of compact ellipsoids on the surface of αCT. In contrast to monolayers with lesser inter-pOEGMA interactions (i.e., in the "free" and loose contact regimes, Figure 2c), the dense brush–ellipsoid monolayers effectively block the passage of biomacromolecules (Supporting Information Figure S4), despite the fact that the length of the backbone is quite low (n < 20–40). The ellipsoidal shape of the pOEGMA chains, as illustrated conceptually in Figure 2c as hexagonally packed hard circles, yield a comparatively small barrier to permeation by small molecules, likely due to the presence of finite gaps within monolayer between polymer chains. Such gaps are observed in the 2D hexagonal packing of non-interpenetrated circles and can account for down to ≈9% of the surface area.[14] The gaps should be smallest just prior to the transition of the pOEGMA chains from ellipsoids to cylinders (i.e., strongest inter-polymer interactions), and is consistent with the maximum preferential activity towards small substrates observed in this region. By changing conformation from ellipsoidal to cylindrical, the inter-penetration of polymer side-chains closes these gaps, thus yielding an effective diffusion barrier to small and large molecules alike, as a function of their hydrodynamic radius.

The pOEGMA monolayers in the "free" and loose contact regime were obtained at low grafting densities and mainly when the side-chains were short (m ≤ 4–5). For these more disordered monolayers, trends comparable to those observed for linear polymers were observed. That is, permeability towards small and large molecules alike was restricted with increasing grafting density and pOEGMA backbone length.[15] The lack of significant preferential activity towards small molecule substrates is consistent with the observations made with a conjugate of αCT bearing 9–10 chains of linear 5 kDa PEG chains (≈1.8 for BT*p*NA ÷ casein and ≈1.2 for peptide ÷ casein; Supporting Information Table S9). It should be noted that higher degrees of modification with linear PEG were not possible. Protein-bound linear PEG is expected to adopt a random-coil or a mushroom conformation depending on grafting density.[16] Assuming αCT to be a sphere with a 2-nm radius,[17] the brush–ellipsoid regime was observed at grafting densities of one pOEGMA chain per 4.2–6.3 nm^2 (x = 12 and 8, respectively) in combination with m ≥ 8–10 and n ≤ ≈35–40. These guidelines, in combination with analysis by ^{1}H NMR spectroscopy (when possible for soluble conjugates), should be used to prepare molecular sieving coatings for other applications.

5. Molecular Sieving for "smart" PEGylation

In addition to the comb polymers discussed above, other architecturally complex polymers such as double-branched PEG, polysaccharides, and hyperbranched polymers have shown beneficial properties for the modification of proteins.[15,18] Unfortunately, little systematic modulation of the structure of these polymers has been examined. In a recent study, Wurm et al.[18] have observed only a small effect of polymer architecture on bioactivity within a library of hyperbranched poly(glycerol)–protein conjugates. In their study however, grafting density is quite low and their findings corroborate those herein at low grafting densities. It therefore appears evident that manifestations of polymer architecture on protein bioactivity only become pronounced at very high grafting densities, where inter-polymer interactions direct organization of the polymer within the monolayer.

To assess the usefulness of specific zones within the conformation diagram of protein-bound pOEGMA monolayers for the PEGylation of proteins, the catalytic activity of selected conjugates towards BT*p*NA was measured in the presence of α_1-antichymotrypsin (α_1-antiCT), a competitor for the active catalytic site on the protein.[19] This glycoprotein is known to bind αCT in a strong 1:1 complex devoid of catalytic activity and was used herein to simulate recognition by biomacromolecules, such as immune system components or proteases. As seen in **Figure 4**, one equivalent of α_1-antiCT completely inhibited the

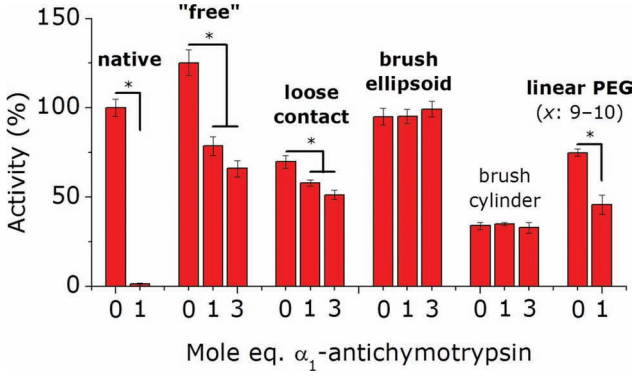

Figure 4. "Molecular sieving" for "smart" PEGylation of proteins. The competition of α_1-antiCT for the active site of αCT was examined as model for recognition by biomolecules such as immune system components. The inhibitory effect of α_1-antiCT was observed for all αCT–polymer conjugates, except for those within the brush regime. The conjugate in the brush–ellipsoid regime possessed the full catalytic activity of the native enzyme, despite being modified with 12 polymer chains. Mean ± SD (n = 3). Samples analyzed: "free" (x = 4, n = 25, m = 8–10); loose contact (x = 12, n = 35, m = 4–5); brush–ellipsoid (x = 12, n = 25, m = 8–10); brush–cylinder (x = 12, n = 55, m = 8–10). (Star denotes statistically significant difference at p = 0.05). x is the grafting density of the polymer on the surface of the protein.

activity of the native enzyme. As α_1-antiCT is a large molecule (≈68 kDa), it was rationalized that the polymer monolayers could, in certain conformations, selectively block this protein, while nevertheless admitting a small molecule substrate to the active site of αCT. Four αCT–pOEGMA conjugates were selected from within different parts of the conformational diagrams above as representative of "free", loose contact, brush–ellipsoid, and brush–cylinder regimes (see figure caption for specific *x*, *n*, *m* of the conjugates). Based on the results from the previous sections, the first two conjugates were expected to be sensitive to α_1-antiCT while the latter two not. The results presented in Figure 4 confirm this expectation. Remarkably, due to the "molecular sieving" effect discussed above, the conjugate in the brush–ellipsoid regime displayed ≈100% of the catalytic activity of the native enzyme, despite the fact that it bore 12 polymer chains, and was completely insensitive to α_1-antiCT. The conjugate in the brush–cylinder regime displayed similar properties, but had lower activity due to closure of the gaps between the POEGMA chains. These results corroborate similar findings from above (Figure 3).

As a control, a conjugate of αCT bearing 8–9 linear chains of PEG also showed a marked decrease of activity upon addition of as little as 1 eq. of α_1-antiCT (Figure 4). Comparable results were observed for the other two substrates (Supporting Information Figure S6). It should be noted that the activity of certain conjugates towards BT*p*NA was higher than 100%. This phenomenon has been previously reported for trypsin as resulting from a micro-environmental effect.[20] These combined results indicate protein-bound pOEGMA monolayers within the brush–ellipsoid conformation are of significant interest for the PEGylation of proteins whose activity involves small molecules, which includes the ever expanding list of anticancer enzymes.[2a] It should be noted that some of the enzymatic activity tests were performed in the presence of small amounts of organic solvent (DMF, DMSO; for substrate solubility), which may potentially influence polymer conformation. Nevertheless, the correspondence between transitions observed in the activity maps (Figure 3) and polymer conformation (in pure aqueous media, Figure 2b), in addition to the corroborating evidence for molecular sieving from Figure 4, appears to rule out a strong influence of these amounts of organic solvent on the results presented.

6. Temperature-Induced Conformational Changes to Protein-Bound pOEGMA

pOEGMA is a thermo-sensitive polymer[6b] that undergoes a coil to globule transition at a temperature known as the cloud-point, which is influenced by the length of the side-chain *m*, though not that of the backbone,[6b,21] and concentration.[21] To rule out the influence of thermo-sensitivity on the transitions observed above, the cloud-points of all conjugates were measured. This was deemed particularly necessary considering that the high grafting density of pOEGMA on the protein creates an artificially high local concentration of polymer, which should depress the cloud-point of these polymers significantly, as observed on particle surfaces elsewhere.[22] Stimuli-sensitive protein–polymer conjugates are notably receiving increasing interest in a variety of fields.[23] The cloud-points measured for the conjugates were consistent with those previously reported for pOEGMA in solution[6b,21] (Supporting Information Table S10 and **Figure 5**a) and were all well above 37 °C, with the exception of αCT–pOEGMA conjugates with *m* = 2, which had cloud points ≈20–30 °C. These low values prompted their exclusion from the flexibility analysis shown in Figure 2b owing to possible misinterpretation. Increasing the grafting density of αCT–pOEGMA conjugates (*m* = 8–10) from *x* = 2 to 12 lead to an impressive depression of the cloud-point by ≈20 °C (Figure 5b), confirming the high local concentration of pOEGMA on the surface of αCT.[21] Overall, the thermo-sensitivity of pOEGMA can be ruled out as cause for the transitions observed in Figure 2b.

7. Conclusions

This work constitutes the first elucidation of the conformation/permeability diagram of protein-bound pOEGMA monolayers

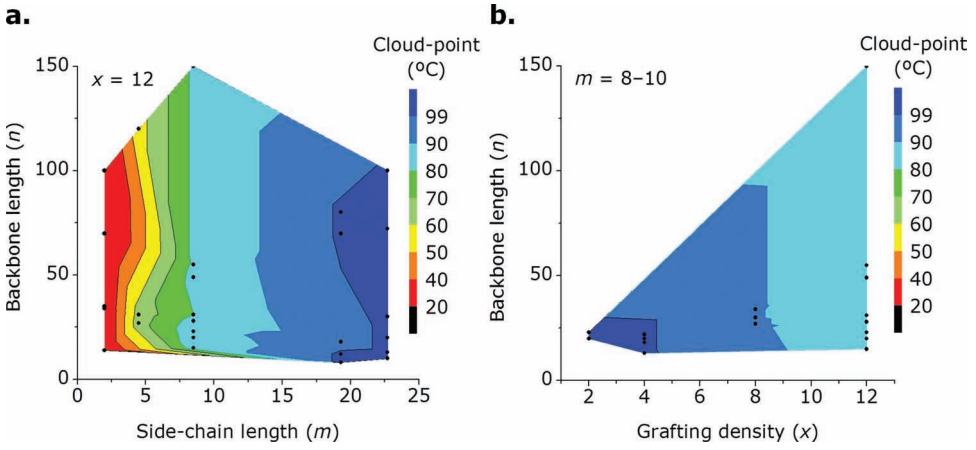

Figure 5. Thermo-sensitivity of αCT–pOEGMA conjugates. a) The cloud-point of αCT–pOEGMA conjugates decreased with increasing *m*, though was largely independent of *n*. b) The cloud-point of αCT–pOEGMA conjugates decreased with grafting density *x*. Color maps established as linear projections between data-points (black dots are the mean of n = 3).

and provides a detailed and systematic investigation of how the aspect ratio of protein-tethered polymers can be modulated to predictably tune protein bioactivity. ^{1}H NMR spectroscopy was a simple, rapid, and accessible tool for screening the conformational state of protein-bound pOEGMA. As the permeability of most pOEGMA monolayers cannot be analyzed in the same fashion as for αCT herein (i.e., due to a lack of substrates of differing size), NMR spectroscopy should serve as a tool of importance for directing monolayer design towards the brush–ellipsoid regime through the flexibility factor *F*. This regime showed a not previously described molecular sieving effect which is inaccessible using other modern PEGylation strategies or using conventional linear polymers.[15,24] This study points notably to the importance of grafting density and opens the door for more systematic evaluations of surface-bound polymer monolayers with complex architectures. The guidelines established herein may be applicable to other proteins for the development of new optimized therapeutic agents and stress the yet largely untapped parameter of polymer architecture in bioconjugate design. In addition, the same guidelines provide insight into the design of other functional coatings with selective permeability to small molecules for wide-ranging applications in the biomedical field.

8. Experimental Section

Materials: 2-Amino-2-hydroxymethyl-propane-1,3-diol (Tris), calcium chloride, α-chymotrypsin (αCT) from bovine pancreas, α_1-antichymotrypsin (human), sodium phosphate dibasic anhydrous and di-sodium hydrogen phosphate were purchased from AppliChem (Axon Lab AG) and used as received. 2,2′-bipyridine, 2-bromoisobutyryl bromide, copper(I) bromide, copper(II) bromide, α-cyano-4-hydroxycinnamic acid, dithiothreitol (DTT), guanidinium HCl, iodoacetamide, milk casein (sodium salt), *N*-benzoyl-L-tyrosine *p*-nitroanilide (BT*p*NA), *N*-succinyl-Ala-Ala-Pro-Phe *p*-nitroanilide, oligoethylene glycol monomethyl ether methacrylate (OEGMA; average M_n: 188, 300, 475, 950, 1100 Da), pepsin (2188 U mg^{-1} protein), sinapinic acid, trichloroacetic acid, trifluoroacetic acid (TFA), and trypsin were purchased from Sigma-Aldrich (Buchs, Switzerland) and used as received. Deuterium Oxide was purchased from Cambridge Isotope Laboratories and used as received. All solvents were of the purest grade available.

Equipment: Organic analytical size-exclusion chromatography (SEC) measurements were performed in DMF containing 0.01 M LiBr using a Viscotek TDAmax system (Viscotek, Houston, TX) equipped with a differential refractive index detector, a low-angle light-scattering detector, and a right-angle light-scattering detector. Absolute molecular weights were reported. Separation was achieved using two Viscotek columns (CLM 3047) in series at a flow rate of 1 mL min^{-1} at 45 °C. Aqueous SEC measurements were performed in 100 mM phosphate buffer (pH = 6.8) using a Viscotek TDAmax system (Viscotek, Houston, TX) equipped with differential refractive index detector, a low-angle light-scattering detector, and a right-angle light-scattering detector. Absolute molecular weights were reported. Separation was achieved using three Viscotek columns (CLM 3016) in series at a flow rate of 0.7 mL min^{-1} at 35 °C. Activity tests were conducted using an Infinite M200 microplate reader (Tecan Ltd.). An Ultrafextreme instrument (Bruker) was used in linear mode for MALDI-TOF MS analysis.

Preparation of αCT Macro-Initiators: αCT macro-initiators were prepared following a modified procedure from Lele et al.[9a] αCT (500 mg, 0.02 mmol of protein; 0.28 mmol of ε-NH_2 groups in lysine residues) was dissolved in 100 mM phosphate buffer (50 mL, pH 8). An appropriate amount of 2-bromoisobutyryl bromide (10–250 eq. relative to protein) dissolved in chloroform was added drop-wise to the vigorously stirred enzyme solution. The mixture was allowed to react at 4 °C for 30–150 min and the pH of the reaction mixture was maintained at 7.5–8 by addition of 100 mM NaOH. The degree of modification was altered by changing the concentration of 2-bromoisobutyryl bromide. After reaction, the solution was centrifuged to remove any precipitate and then the activated proteins were purified by preparative SEC (Sephadex G-25) followed by centrifugal dialysis against water for (MWCO 10 kDa). Purified αCT macro-initiators were isolated by freeze-drying and stored at –20 °C until used. To determine the number of initiators covalently connected to αCT, the purified macro-initiators were dissolved in 50 μL water containing 0.1% TFA. 1 μL of this solution was mixed with 1 μL of matrix (saturated sinapinic acid in 50% acetonitrile containing 0.1% TFA), the mixture spotted on the target, and then analyzed by MALDI TOF MS using α-cyano-4-hydroxycinnamic acid as matrix (≈5 mg mL^{-1} in 50% acetonitrile containing 0.1% TFA); Figure 1b. The average number of initiators present was determined by dividing the increase of molecular weight relative to the native protein by 150 Da, the molecular weight of the initiating group. Selected samples were also dissolved in acetonitrile:water 1:1 (v/v) and analyzed by nano-electrospray mass spectrometry, which yielded comparable results to those obtained by MALDI TOF MS. Good control over the grafting density was achieved by controlling the amount of acylating agent added (Supporting Information Figure S1).

Analysis of Location of Initiator Groups by Tryptic Digestion/Mass Spectrometry: Tryptic digestion LC-MS was performed under contract by the *Protein Analysis Group* at the *Functional Genomics Center Zurich*. Native αCT and αCT macro-initiators (≈0.1 mg) were dissolved in 20 μL 6 M guanidinium HCl (pH 8) and then 2 μL 500 mM DTT was added. The mixture was incubated at 37 °C for 1 h. To the reduced samples, 1.5 μL iodoacetamide was added and the mixture left in the dark for 30 min at 37 °C. 10 μL of the solution of alkylated protein was then added to 450 μL buffer (10 mM Tris, 2 mM $CaCl_2$, pH 8.2), 100 μL trypsin (0.01 μg μL^{-1} in 10 mM Tris, 2 mM $CaCl_2$, pH 8.2), and 60 μL acetonitrile. The digestion was allowed to proceed for 2 h at 50 °C. The digested samples were analyzed by MALDI TOF MS using α-cyano-4-hydroxycinnamic acid as matrix (5 mg mL^{-1} in 50% acetonitrile containing 0.1% TFA). Despite careful comparative analysis of sequence coverage between the native and a sparingly modified αCT derivative (x = 2), dominant fragments unambiguously modified with 2-bromoisobutyryl bromide were not found. This result points to a random distribution of initiator groups on αCT rather than the preferential modification of specific locations on the protein.

In Situ Growth of Polymer Chains from αCT Macro-Initiators: Atom transfer radical polymerization (ATRP) was used to grow pOEGMA chains from the αCT macro-initiators in a modified procedure from Lele et al.[9a] In a typical reaction, 50 mg of αCT macro-initiator (0.002 mmol protein; 0.004 mmol initiators, 1 eq.) and OEGMA (0.4 mmol, 100 eq.) were placed in a sealed round-bottom flask containing 15 mL 100 mM phosphate buffer (pH 6) and the solution de-oxygenated under a flow of argon. This solution was transferred to a second sealed flask containing CuBr (2.9 mg, 0.02 mmol, 5 eq.), $CuBr_2$ (4.4 mg, 0.02 mmol, 5 eq.), and 2,2′-bipyridine (9.4 mg, 0.06 mmol, 15 eq.) to initiate the polymerization reaction. The polymerization was allowed to proceed at 4 °C, and at given time points aliquots were extracted using degassed syringes. The aliquots were exposed to air to quench the polymerization reaction and diluted in D_2O to measure monomer conversion by ^{1}H NMR spectroscopy (Figure 1c). After analysis by ^{1}H NMR spectroscopy, the αCT–pOEGMA conjugates were purified by centrifugal dialysis (MWCO 30 kDa). When the expected molecular weight of the conjugate was below 30 kDa, purification was achieved by silica gel chromatography. The complete numerical characteristics of all αCT–pOEGMA conjugates (x, m, n) are listed in Supporting Information Table S1–S8.

Analysis of Molecular Weight of αCT–pOEGMA Conjugates: Owing to the difficulty in analyzing the molecular weight of protein–polymer conjugates, this parameter was determined by three complementary techniques: ^{1}H NMR spectroscopy, SEC, and by UV-vis spectrometry. The molecular weights determined by these methods are listed in Supporting Information Table S1–S9 at the end of this document. ^{1}H

NMR spectroscopy: Because characteristic peaks of αCT could not be observed in the ^{1}H NMR spectra of purified αCT–pOEGMA conjugates, the molecular weight of the latter was determined based on monomer conversion and the known initial ratio of αCT to OEGMA; SEC: The molecular weight and molecular weight distribution of αCT–pOEGMA was analyzed by aqueous SEC for conjugates with $m \geq 4$–5, whereas conjugates with shorter m were analyzed by SEC in DMF. Typical chromatograms are shown in Figure 1d. UV-vis spectroscopy: The molecular weight of αCT–pOEGMA was determined by dissolving known amounts of purified conjugates in distilled water, and then determining the concentration of αCT in this solution by measuring the absorbance at 280 nm. pOEGMA does not absorb significantly at this wavelength and thus does not interfere with quantification of molecular weight in this manner. All three analytical techniques yielded comparable values of molecular weight.

Analysis of Initiation Efficiency of αCT Macro-Initiators: To analyze the efficiency of the initiation process, the molecular weight of the individual pOEGMA chains were analyzed after digestion of a conjugate by pepsin. This enzyme is known to hydrolyze amide bonds, but not affect ester bonds. Indeed, incubation of 10 mg of free pOEGMA (i.e., not attached to a peptide or protein) in 3 mL 100 mM citric acid buffer (pH 3) with 2 mL of pepsin (5 mg mL^{-1} in 100 mM citric acid buffer, pH 3) at 37 °C over a 24 h period did not alter the SEC chromatogram of this polymer (Supporting Information Figure S2a). In contrast, over a 70 h period, the peak in the SEC chromatogram of a selected αCT–pOEGMA (*x*, *m*, *n*: 4, 8–10, 80), which was pre-denatured at 95 °C for 10 min, shifted to lower molecular weight and remained monomodal (Supporting Information Figure S2b). The molecular weight of the digested peak corresponded to the value expected for initiation at all possible groups on the protein. These results point to quasi-unitary efficiency of initiation. The polymer chains should all have comparable lengths (*n*) within a given conjugate.

Preparation of αCT–(linear PEG) Conjugates: Conjugates of αCT with linear PEG were prepared by reaction of αCT with monomethoxy polyethylene glycol (5 kDa; $mPEG_{5kDa}$) bearing an aldehyde (CHO) functional group. For reductive alkylation, αCT (2 mg, 0.08 μmol, 1 eq.) and $mPEG_{5kDa}$-CHO (50 mg, 0.01 mmol, 125 eq.) were dissolved in 1 mL 100 mM phosphate buffer (pH 6) containing 20 mM $NaCNBH_4$. The reaction was allowed to proceed for 16 h at 4 °C. After the conjugation reaction, the conjugate was purified by centrifugal dialysis (MWCO 30 kDa) and the number of conjugated polymer chains determined as for the αCT–pOEGMA conjugates.

^{1}H NMR Spectroscopy: ^{1}H NMR spectra were recorded in D_2O on a Bruker Av400 spectrometer (Bruker BioSpin, Fällanden, Switzerland) operating at 400 MHz for protons. Each spectrum consisted of 512 scans, with an acquisition time of 4 s per scan (conventional parameters for small-molecules).

Thermo-Sensitivity of αCT–pOEGMA Conjugates: Solutions of conjugates (5 mg mL^{-1} total) in phosphate buffered saline (pH 7.4) were prepared and the cloud-point measured using an Optimelt MPA100 system (Stanford Research Systems). The recorded turbidity curve was normalized between 0 and 1 and the transition temperature defined as that corresponding to a normalized absorbance of 0.5 (Supporting Information Table S10). A constant heating rate of 1 °C min^{-1} was used in all experiments. Equipment used was supported by Advantage West Midlands and part funded by the European Regional Development Fund.

Enzymatic Activity of αCT–Polymer Conjugates: The enzymatic activity of the conjugates was measured towards three substrates (Supporting Information Table S1–S9 and Figure S4). Benzoyl-L-tyrosine *p*-nitroanilide (BT*p*NA): to solutions of αCT or αCT–polymer conjugates (0.1 mg mL^{-1} protein) in 200 μL 100 mM Tris buffer (pH 8) in a 96-well plate was added 50 μL of a solution of BT*p*NA (1 mg mL^{-1}) in DMF at room temperature or 37 °C. The evolution of absorbance at 412 nm was recorded over 3 min and the activity calculated from the initial slope. *N*-succinyl-L-Ala-L-Ala-L-Pro-L-Phe-*p*-nitroanilide: to solutions of αCT or αCT–polymer conjugates (0.01 mg mL^{-1} protein) in 100 μL 100 mM Tris buffer (pH 8) in a 96-well plate was added 25 μL of a solution of substrate (1 mg mL^{-1}) in DMSO at room temperature or 37 °C. The evolution of absorbance at 412 nm was recorded over 1 min and the activity calculated from the initial slope. Milk casein: to solutions of αCT or αCT–polymer conjugates (0.1 mg mL^{-1} protein) in 100 μL 100 mM Tris buffer (pH 8) in Eppendorf vials was added 1 mL of a casein suspension (10 mg mL^{-1}) and the mixture incubated at room temperature or 37 °C. After 20 min, the reaction was stopped with 200 μL of 50% trichloroacetic acid in water. The precipitate was removed by centrifugation at 4 °C and the absorbance of 200 μL of supernatant at 280 nm measured.

Inhibition Assay with α_1-antiCT: To assess the sensitivity of αCT and αCT–polymer conjugates towards inhibition by α_1-antiCT, the enzymatic activity of αCT and αCT–polymer conjugates was measure as above, in the presence of 1–3 molar eq. α_1-antiCT (added sample solution prior to substrate). Results for peptide and casein substrate are found in Supporting Information Figure S6.

Statistics: The activity of αCT–polymer conjugates were compared by one-way ANOVA followed by a Tukey post-hoc test. Differences were considered significant at $p < 0.05$.

Acknowledgements

M.L. recognizes a doctoral scholarship from the Chinese Scholarship Council (CSC). M.I.G. recognizes funding from HEFCE. D.J.P. recognizes a scholarship from the University of Warwick. Expert technical assistance from the Functional Genomics Center Zurich and funding from the Sassella foundation are gratefully acknowledged.

Received: August 7, 2012
Revised: October 17, 2012
Published online: November 15, 2012

[1] a) T. M. Allen, P. R. Cullis, *Science* **2004**, *303*, 1818; b) S. Shaunak, A. Godwin, J. W. Choi, S. Balan, E. Pedone, D. Vijayarangam, S. Heidelberger, I. Teo, M. Zloh, S. Brocchini, *Nat. Chem. Biol.* **2006**, *2*, 312; c) Y. Yamamoto, Y. Tsutsumi, Y. Yoshioka, T. Nishibata, K. Kobayashi, T. Okamoto, Y. Mukai, T. Shimizu, S. Nakagawa, S. Nagata, T. Mayumi, *Nat. Biotechnol.* **2003**, *21*, 546; d) K. Fuhrmann, J. D. Schulz, M. A. Gauthier, J.-C. Leroux, *ACS Nano* **2012**, *6*, 1667; e) J. J. Moon, H. Suh, A. Bershteyn, M. T. Stephan, H. Liu, B. Huang, M. Sohail, S. Luo, S. Ho Um, H. Khant, J. T. Goodwin, J. Ramos, W. Chiu, D. J. Irvine, *Nat. Mater.* **2011**, *10*, 243; f) A. Hucknall, D. H. Kim, S. Rangarajan, R. T. Hill, W. M. Reichert, A. Chilkoti, *Adv. Mater.* **2009**, *21*, 1968; g) A. Hucknall, S. Rangarajan, A. Chilkoti, *Adv. Mater.* **2009**, *21*, 2441; h) H. Ma, J. Hyun, P. Stiller, A. Chilkoti, *Adv. Mater.* **2004**, *16*, 338; i) P. Akcora, H. Liu, S. K. Kumar, J. Moll, Y. Li, B. C. Benicewicz, L. S. Schadler, D. Acehan, A. Z. Panagiotopoulos, V. Pryamitsyn, V. Ganesan, J. Ilavsky, P. Thiyagarajan, R. H. Colby, J. F. Douglas, *Nat. Mater.* **2009**, *8*, 354; j) M. A. C. Stuart, W. T. S. Huck, J. Genzer, M. Muller, C. Ober, M. Stamm, G. B. Sukhorukov, I. Szleifer, V. V. Tsukruk, M. Urban, F. Winnik, S. Zauscher, I. Luzinov, S. Minko, *Nat. Mater.* **2010**, *9*, 101.

[2] a) G. Pasut, M. Sergi, F. M. Veronese, *Adv. Drug Delivery Rev.* **2008**, *60*, 69; b) G. Pasut, F. M. Veronese, *Adv. Drug Delivery Rev.* **2009**, *61*, 1177.

[3] C.-H. Pui, W. E. Evans, *N. Engl. J. Med.* **2006**, *354*, 166.

[4] J. D. Broome, *Nature* **1961**, *191*, 1114.

[5] L. Feuz, P. Strunz, T. Geue, M. Textor, O. Borisov, *Eur. Phys. J. E: Soft Matter Biol. Phys.* **2007**, *23*, 237.

[6] a) J.-F. Lutz, J. Andrieu, S. Üzgün, C. Rudolph, S. Agarwal, *Macromolecules* **2007**, *40*, 8540; b) J. F. Lutz, O. Akdemir, A. Hoth, *J. Am. Chem. Soc.* **2006**, *128*, 13046.

[7] a) W. Gao, W. Liu, J. A. Mackay, M. R. Zalutsky, E. J. Toone, A. Chilkoti, *Proc. Natl. Acad. Sci. USA* **2009**, *106*, 15231;

b) S. M. Ryan, X. Wang, G. Mantovani, C. T. Sayers, D. M. Haddleton, D. J. Brayden, *J. Controlled Release* **2009**, *135*, 51; c) J. P. Magnusson, S. Bersani, S. Salmaso, C. Alexander, P. Caliceti, *Bioconjugate Chem.* **2010**, *21*, 671; d) W. Gao, W. Liu, T. Christensen, M. R. Zalutsky, A. Chilkoti, *Proc. Natl. Acad. Sci. USA* **2010**, *107*, 16432; e) L. Tao, G. Mantovani, F. Lecolley, D. M. Haddleton, *J. Am. Chem. Soc.* **2004**, *126*, 13220; f) G. Mantovani, F. Lecolley, L. Tao, D. M. Haddleton, J. Clerx, J. J. L. M. Cornelissen, K. Velonia, *J. Am. Chem. Soc.* **2005**, *127*, 2966; g) M. A. Gauthier, M. Ayer, J. Kowal, F. R. Wurm, H.-A. Klok, *Polym. Chem.* **2011**, *2*, 1490.

[8] G. Cheng, Y. B. Melnichenko, G. D. Wignall, F. J. Hua, K. Hong, J. W. Mays, *Macromolecules* **2008**, *41*, 9831.

[9] a) B. S. Lele, H. Murata, K. Matyjaszewski, A. J. Russell, *Biomacromolecules* **2005**, *6*, 3380; b) S. Averick, A. Simakova, S. Park, D. Konkolewicz, A. J. D. Magenau, R. A. Mehl, K. Matyjaszewski, *ACS Macro Lett.* **2011**, *1*, 6.

[10] K. Matyjaszewski, N. V. Tsarevsky, *Nat. Chem.* **2009**, *1*, 276.

[11] L. A. Lokshina, V. N. Orekhovich, V. A. Sklyankina, *Nature* **1964**, *204*, 580.

[12] J. Spěváček, *Curr. Opin. Colloid Interface Sci.* **2009**, *14*, 184.

[13] D. Dukes, Y. Li, S. Lewis, B. Benicewicz, L. Schadler, S. K. Kumar, *Macromolecules* **2010**, *43*, 1564.

[14] A. Donev, F. H. Stillinger, P. M. Chaikin, S. Torquato, *Phys. Rev. Lett.* **2004**, *92*, 255506.

[15] M. A. Gauthier, H.-A. Klok, *Polym. Chem.* **2010**, *1*, 1352.

[16] S. S. Pai, B. Hammouda, K. Hong, D. C. Pozzo, T. M. Przybycien, R. D. Tilton, *Bioconjugate Chem.* **2011**, *22*, 2317.

[17] P. V. Kostetsky, *Biochemistry* **2007**, *72*, 392.

[18] F. Wurm, C. Dingels, H. Frey, H.-A. Klok, *Biomacromolecules* **2012**, *13*, 1161.

[19] B. S. Cooperman, E. Stavridi, E. Nickbarg, E. Rescorla, N. M. Schechter, H. Rubin, *J. Biol. Chem.* **1993**, *268*, 23616.

[20] Z. Ding, G. Chen, A. S. Hoffman, *J. Biomed. Mater. Res.* **1998**, *39*, 498.

[21] K. Bebis, M. W. Jones, D. M. Haddleton, M. I. Gibson, *Polym. Chem.* **2011**, *2*, 975.

[22] M. I. Gibson, D. Paripovic, H.-A. Klok, *Adv. Mater.* **2010**, *22*, 4721.

[23] A. Nelson, *Nat. Mater.* **2008**, *7*, 523.

[24] a) S. Brocchini, A. Godwin, S. Balan, J.-W. Choi, M. Zloh, S. Shaunak, *Adv. Drug Delivery Rev* **2008**, *60*, 3; b) M. W. Popp, S. K. Dougan, T. Y. Chuang, E. Spooner, H. L. Ploegh, *Proc. Natl. Acad. Sci. USA* **2011**, *108*, 3169.